Lehigh University

INSTITUTE OF RESEARCH

Welded Continuous Frames & Their Components

Progress Report T

BUCKLING OF STEEL ANGLES IN THE PLASTIC RANGE

by

BRUNO THÜRLIMANN and GEERHARD HAAIJER

(Not for Publication)

WELDED CONTINUOUS FRAMES AND THEIR COMPONENTS

Progress Report T

BUCKLING OF STEEL ANGLES IN THE PLASTIC RANGE

By

Bruno Thurlimann

Geerhard Haaijer

(Not for Publication)

This work has been carried out as a part of an investigation sponsored jointly by the Welding Research Council and the Department of the Navy with funds furnished by the following:

American Institute of Steel Construction
American Iron and Steel Institute
Institute of Research, Lehigh University
Column Research Council (Advisory)
Office of Naval Research (Contract No. 39303)
Bureau of Ships
Bureau of Yards and Docks

Fritz Engineering Laboratory
Department of Civil Engineering and Mechanics
Lehigh University
Bethlehem, Pennsylvania

August 15, 1953

Fritz Laboratory Report No. 205E-3

TABLE OF CONTENTS

	Page
INTRODUCTION	1
I. Experimental Investigation	2
1. Test Program	2
2. Testing Procedure	3
3. Test Results	5
II. Theoretical Investigation	7
1. Yielding of Mild Steel	7
2. Buckling of Columns in the Plastic Range	8
a. Simply Supported Column	9
b. Fixed-Ended Column	12
3. Torsional Buckling of Angles in the Plastic Range	14
4. Comparison with Plastic Buckling Theories	19
ACKNOWLEDGEMENTS	22
List of References	23
Tables I and II	
Figures 1 to 17	

Buckling of Steel Angles in the Plastic Range

INTRODUCTION

It is well known that the cross sectional dimensions of the commonly rolled WF- and I- Beams are such that local buckling of their flanges and webs will not occur if they are stressed within the elastic range. However, a number of tests conducted at Fritz Engineering Laboratory and other places on the ultimate load carrying capacity of structural steel beams and frames, showed that local buckling may occur in the plastic range such that the ultimate load does not reach the value predicted by simple plastic analysis. Hence it became necessary to study this problem. A research program was proposed in Progress Report Q (1)*. Its aim was stated "to establish a specification for the required geometric projection of I- and WF- shapes so that plastic hinges can be developed and maintained through a considerable range of rotation without reduction due to local buckling".

Presently, theories dealing with plastic buckling of plates can be arranged in 3 groups connected with the names of Bijlaard - Ilyushin - Stowell, Handelman - Prager and Bleich respectively (2), (3), (4). However, test results on plates of structural steel of the A-7 type, having a very pronounced yield level of a considerable extent, were not available to make any critical comparison with these theories. Hence it was decided to make a few simple tests on specimens of structural steel and

* See list of references at the end of report.

to compare the results with these theoretical predictions. As no satisfactory agreement could be established further theoretical investigations of the problem became necessary. The present paper reports on these tests and discusses a few theoretical studies which have been carried out on buckling of steel columns and plates in the plastic range.

I. Experimental Investigation

1. Test Program:

The test program was conceived with the intension to check the validity of the advanced theories (2), (3), (4) with a few simple and easily controllable tests. Special consideration was given to the theory of Stowell (2), since this theory showed excellent agreement with tests on plates of aluminum alloy 24S-T conducted by the NACA a few years ago (2).

Annealed angle specimens of A-7 steel were chosen for the following reasons:

1. Testing of such specimens can be carried out easily by axial compression in a standard testing machine.
2. The legs of an angle correspond to the outstanding flanges of WF- and I- Beams if the action of the web on the flanges is neglected. Hence the tests may give already certain data as to the behavior of such flanges.
3. Annealing releases the residual stresses due to cooling and other effects. The material will therefore more closely approach the assumption of homogeneity made in all theories.

4. An angle having equal legs can be considered as consisting of 2 long plates, free along one edge and simply supported along the heel (no interaction between the legs). The analysis of such a specimen is greatly simplified due to the fact that the boundary conditions are well defined.

5. The predictions of the buckling load of such specimens by the different theories show wide differences. The tests will throw some light on their validity.

The specimens were prepared from an angle 6 x 6 x 3/8 (14.9 lb.). Their dimensions are given in Table I. The length L was chosen such that their ratios L/r were about 25 (r = radius of gyration). This ratio was low enough ($L/r \leq 30$ for fixed ended columns) such that bending would not occur before the strains reached the strain hardening range. The b/t ratios (width / thickness of leg) was determined on the basis of Stowell's theory such that for b/t = 12.6, 8.8 and 5.25 torsional buckling should occur at a critical strain $\varepsilon_{cr} = 3.45 \cdot 10^{-3}$, $6.10 \cdot 10^{-3}$ and $13.0 \cdot 10^{-3}$ respectively (see Fig. 17). For each b/t - ratio two specimens were prepared.

After completion of this program two tests on specimens of as-delivered material were added to investigate a possible difference in behavior.

2. Testing Procedure:

The annealed specimens were placed in a screw-type testing machine (Fig. 1). Alinement was checked by SR-4 gages placed at mid-length of the specimens. After proper alinement was established the spherical bearing block under the upper head of the machine was locked such that the ends of the specimens

were completely fixed (except for specimen A-42 which was the first one tested).

The total shortening ΔL of the specimen and hence the mean strain $\Delta L/L$ were measured by 3 dial gages. SR-4 gages of 1" and 6 " length (A-11 and A-9) measured the local strains along the flanges. 3 different methods were used to detect torsional buckling:

1. A special "Buckling Detector" was built (Fig. 1). Two aluminum bars placed along the flanges were interconnected by steel springs such that they pressed slightly against them. SR-4 gages placed on the springs picked up the spreading of the bars when buckling of the flanges occurred.
2. Two SR-4 gages placed on the toe of the flange opposite to each other will indicate equal strains as long as the specimen stays straight. If torsional buckling takes place the flange will bend and the SR-4 gages will indicate it by a difference in strain. This method, named "Strain Deviation", was used also.
3. If torsional failure takes place the angle will twist around its heel. A dial measuring this rotation will indicate the beginning of buckling. The test results which are shown subsequently showed that this rotation measurement was in almost all cases the most sensitive indication and gave the most reliable results.

The actual testing was done by applying a chosen strain to the specimen. After the load had settled to a constant value all readings were taken. Thereupon the following strain increment was applied.

The two specimens of "as-delivered" material were tested in a hydraulic testing machine. In such a machine the application of a chosen strain is somewhat more difficult to achieve once the specimen is stressed into the plastic range. Nevertheless the same procedure as before was followed.

3. <u>Test Results</u>:

The test results of all 8 specimens are summarized in Table II. Fig. 3 to 7 are graphical representations of some pertinent measurements.

Fig. 3 shows stress strain curves obtained from coupon tests. The tension coupons "T" were of standard size (ASTM-E8) the compression coupons "C" measured 2 x 1/2 x 3/8" (thickness of angle). The scatter of the results is quite remarkable, especially concerning the strain ε_{st} at which strain hardening starts and the Tangent Modulus E_{st} at the start of the strain hardening range. The values of E_{st} were obtained by plotting the stress-strain curve to a large scale. Furthermore the yield stresses of the coupons are considerably above the yield stresses of the angle specimens (compare Fig. 3 and 4).

A plot of the average stress P/A vs the mean strain $\bar{\varepsilon} = \Delta L/L$ of the angle specimens is shown in Fig. 4. Buckling as indicated by rotation measurements is shown by arrows (except for A-21 where rotation was not measured and buckling as detected by SR-4 gages is substituted). These rotation measurements, taken at mid-length of the specimens are given in Fig. 5. The arrows, indicating torsional buckling, were located at points where the rotation starts to increase at a much greater rate than it did originally. The specimen A-41 (b/t = 6.13) never failed in torsion. The same holds for specimen A-42 with an equal b/t - ratio for which no rotation measurement was taken. The "buckling

detector and the strain gages did not reveal any torsional failure. Both specimens bent around their weak axis after being stressed into the strain hardening range (Euler buckling).

The tests brought out a very important fact. Yielding in an axially compressed specimen does not occur more or less homogeneously, i.e. uniformly distributed over the entire length. On the contrary, for the annealed specimens yielding started at the ends and progressed towards the middle. In Fig. 7 the average strain $\varepsilon = \Delta L/L$ and the local strains measured at mid-length of the specimen are equal in the elastic range (line under 45°). There after the average strain increases whereas the local strains stay stationary. This indicates that yielding takes place at the ends. In case of the "as-delivered" specimens a few yield lines appeared first along the entire specimens. From there on yielding concentrated at the ends again. This fact cannot be enough emphasized as it is in direct contradiction to the assumption of "quasi homogeneous" yielding made in all theories of plastic buckling of plates.

Summarizing, the tests allowed the following conclusions:

1. Yielding of the specimens started at both ends. After these parts reached the strain hardening range yielding progressed towards the center. The average strain $\varepsilon = \Delta L/L$ and local strains differed anywhere from the yield strain ε_y to the strain hardening strain ε_{st}. Yielding definitely occurred non-homogeneously.

2. The critical strain ε_{cr} at which torsional buckling of the specimens took place increased with decreasing b/t - ratio. The 3 specimens A-31,-32,-33 with b/t = 8.8 failed right after being strained to the strain hardening range

($\varepsilon_{cr} \cong 13 \cdot 10^{-3}$). A-41 and -42 with b/t = 6.25 showed not any sign of torsional failure. They failed as columns at strains above ε_{st}.

3. A critical comparison of the test results with the predictions of the available theories (Fig. 17) shows marked discrepancies. First qualitatively, yielding did not occur more or less uniformly along the specimens as assumed in all these theories. Secondly, the quantitative differences are very pronounced. In the second part of this report some theoretical investigations of this problem are presented which may be helpful toward its solution.

II. Theoretical Investigation

1. Yielding of Mild Steel:

The following considerations are based on steel exhibiting properties in tension and compression as shown in Fig. 8. Such a stress-strain diagram is quite common for structural steel under a uni-axial stress. It must be kept in mind that that the strain represents an average strain over a certain gage length. It would be entirely erroneous to assume that the local strains within the plastic range from ε_y to ε_{st} are equal to the average strain . Yielding of mild steel occurs in small slip bands (5). Slip takes place in a "jump" such that the strain across such a narrow band jumps from about $1 \cdot 10^{-3}$ to maybe 15 to $20 \cdot 10^{-3}$. The first slip band originates at a weak point in the specimen, due to an inclusion, a stress concentration or other causes of this nature. From there on yielding will spread along the specimen. For more information, reference (5) may be consulted.

This consideration leads to the conclusion that there is no material within the specimen at a strain between the yield strain ε_y and the strain hardening strain ε_{st}. Either the material is still elastic or it reached the strain hardening range already. How important it is to consider these physical facts in stability problems will first be shown for buckling of columns in the plastic range. For, the mathematical complications of this problem can be overcome very easily and furthermore simplifications for this problem can be introduced which will be used later on for the case of the angles.

2. Buckling of Columns in the Plastic Range:

It is well known that the buckling stress σ_{cr} of an axially loaded, pin-ended column is given by [4]

$$\sigma_{cr} = \frac{\pi^2 \tau E}{(L/r)^2} \tag{1}$$

where:

E = Modulus of Elasticity

$\tau = E_t/E$

E_t = Tangent Modulus

L/r = Slenderness Ratio

For a material as shown in Fig. 8, Eq. (1) gives solutions up to the yield stress σ_y = 33,000 psi and a yield strain $\varepsilon_y = 1.1 \cdot 10^{-3}$. The corresponding slenderness ratio L/r is equal to 94.9. Again for $\varepsilon_{cr} = \varepsilon_{st} = 14 \cdot 10^{-3}$, i.e. at the beginning of the strain hardening range, a solution becomes formally possible. For the tangent modulus E_t becomes equal to the strain hardening modulus E_{st}. The values corresponding to this solution are:

$$\varepsilon_{cr} = \varepsilon_{st} = 14 \cdot 10^{-3}$$

$$\sigma_{cr} = 33{,}000 \text{ psi}$$

$$L/r = 15.4$$

Or in words, a column with a slenderness ratio $L/r = 15.4$ may be compressed under a stress equal to the yield stress $\sigma_y = 33{,}000$ psi up to $\varepsilon_{cr} = 14 \cdot 10^{-3}$ before it buckles. Such behavior was actually exhibited in tests reported in Progress Report S [6]. For any slenderness ratio $94.9 > L/r > 15.4$ eq. (1) does not lend itself to a solution. Hence two important questions arise:

1. How does a column of $L/r = 15.4$ overcome the long yield level without buckling?
2. How much strain can a column $94.9 > L/r > 15.4$ undergo before it buckles?

The questions can only be answered if due consideration is given to the manner in which yielding takes place in a uni-axially compressed member. For numerous experiments [5] and especially the tests on the angle specimens reported before showed that yielding starts at one place and spreads after the already yielded zone reached the strain hardening range.

a. <u>Simply Supported Column</u>:

Taking a simply supported column, 3 different manners in which yielding may occur are considered.

1. The column starts to yield at both ends (Fig. 9a), the yielded zones extend over a length ξL. The bending stiffness of the middle part is still given by EI (I = moment of inertia) whereas the one of the end pieces is greatly reduced to $E_{st}I$, E_{st} being the strain hardening modulus. Assuming the column is continuously compressed such that buckling will occur without strain reversal, the buckling condition of such a column with variable bending stiffness

is given by the transcendental equation:*

$$\lambda \tan \frac{\varphi\pi}{\lambda}\xi \tan \varphi\pi(1/2 - \xi) = 1 \quad (2)$$

Where: $\lambda^2 = E_{st}/E$

$\varphi^2 = P_{cr}/P_E$

$P_E = \pi^2 EI/L^2$

P_{cr} = Buckling Load

For given values of $\lambda^2 = E_{st}/E$ and ξ (extension of yielded zones), eq.(2) furnishes by trial and error a value for φ. The buckling load then is given by

$$P_{cr} = \varphi^2 P_E = \varphi^2 \frac{\pi^2 EI}{L^2} \quad (3)$$

If buckling occurs in the plastic range, i.e. between ε_y and ε_{st}, the yield load is equal to the critical load such that the corresponding slenderness ratio L/r can be computed from the following equation:

$$\sigma_{cr} = P_{cr}/A = \sigma_y = \varphi^2 \frac{\pi^2 EI}{(L/r)^2} \quad (4)$$

Furthermore the shortening ΔL and the average strain ε_{cr} at which buckling occurs are of interest. The shortening is equal to:

$$\Delta L = \varepsilon_y \cdot (1-2\xi)\ L + \varepsilon_{st}\ 2\xi L \quad (5)$$

and the average strain:

$$\varepsilon_{cr} = \Delta L/L = (1-2\xi)\,\varepsilon_y + 2\xi\varepsilon_{st} \quad (6)$$

The values given in Fig. 8 were used to derive the curves (a) of L/r vs ξ and $\varepsilon_{cr}/\varepsilon_y$ vs L/r shown in Fig. 11 and 12 respectively.

---

* See reference (7), p. 128. (Some changes in notation have been made.)

2. The other extreme case is to consider yielding starts in the middle of the column and spreads toward the ends (Fig. 9b). Here the column has a greatly reduced bending stiffness over a length $2\xi L$ at mid-length. The equation determining the buckling load is:

$$\tan \frac{\varphi\pi}{\lambda}\xi \tan \varphi\pi(1/2 - \xi) = \lambda \tag{7}$$

Again λ and ξ determine φ such that eq. (7) is fulfilled. Eq.(4) and (6) hold for the critical slenderness ratio L/r and the critical strain ε_{cr} respectively. Curves (b) in Fig. 11 and 12 give the results of such calculations.

3. If yielding takes place quasi-homogeneously yielded strips will form all along the column (Fig. 9c). Material being at E and E_{st} will be distributed more or less uniformly such that the bending stiffness will have an average value $\bar{E}I$, $\bar{E}$ being:

$$\bar{E} = E\,(1-2\xi) + 2\xi E_{st} \tag{8}$$

For $\xi = 0$, $\bar{E} = E$ and for $\xi = 0.5$, $\bar{E} = E_{st}$ as it should be. The critical L/r follows from

$$\sigma_y = \frac{\pi^2\bar{E}}{(L/r)^2} \tag{9}$$

Eq. (6) still applies for the critical strains. Numerical results are plotted as curves (c) in Fig. 11 and 12.

Comparison of the curves (a) to (c) shows great variation in the results. The answer on how such a column will fail actually can only be decided on the basis of test results. Quite possibly there is no unique answer at all as yielding may start almost anywhere along the column.

After the curves presented in Fig. 11 and 12 were worked out, Mr. Paul Paris, research assistant at Fritz Engineering Laboratory, brought to our attention that numerous model tests on simply supported columns had been made by Mr. T. A. Hunter and himself at the University of Michigan under the direction of Professor T. A. Van den Broek. In these tests the axial shortening under increasing axial load P was measured. 37 results are plotted in Fig. 12. Unfortunately the values for E_{st} and ε_{st} of the steel used were not determined. The mean value of the yield stress was about 35,000 psi. Nevertheless it is quite remarkable how consistently the test results lay between curves (a) and (b). If the actual E_{st} and ε_{st} would have been measured and subsequently used to get curves (a) and (b) closer correspondence in the lower L/r range could have been established. In any case the test results show that the assumptions made lead to reasonable results. The third case considered (quasi-homogeneously yielding) leads certainly to too high values (curve (c)). The assumption of yielding spreading from the middle gives conservative results (curve (b)).

b. Fixed-Ended Column:

The 3 cases considered before will again be treated separately

1. The assumption that yielding starts at the ends and spreads over the two lengths ξL (Fig. 10a) leads in case

of the fixed ended column to the following buckling condition:

$$\tan \frac{\varphi\pi}{\lambda}\xi + \tan \varphi\pi\,(1/2 - \xi) = 0 \tag{10}$$

The symbols have the same significance as in the previous equations (2) to (7). The curves (a) in Fig. 13 and 14 were derived from eq.(10), (4) and (5) using the material properties given in Fig. 8.

2. Fig. 10b illustrates the case of yielding spreading from the middle. Eq. (10) applies for this case also. A short consideration of the buckled shape will illustrate this identity. Hence the curves (b) in Fig. 13 and 14 coincide with curves (a).

3. For uniform yielding (Fig. 10c) the effective modulus $\overline{E}$ is given by eq. (8). Due to the fix-ends the critical slenderness ratio of the column is $1/2 \cdot L/r$ such that eq. (9) must be changed to:

$$\sigma_y = \frac{\pi^2 E}{(1/2 \cdot L/r)^2} \tag{11}$$

Curves (c) in Fig. 13 and 14 result from this equation.

Again the manner in which yielding takes place has a marked influence on the results. It can be expected that the scatter of experimental results will be much smaller for the case of fixed-ended columns. For curves (a) and (b), derived under the assumption of yielding spreading from the ends and from the middle respectively, are identical. Unfortunately no test results could be found to make a critical comparison.

An approximation for the first two cases (curve (a) and (b)) can readily be derived. Later on use of it will be made for the case of torsional buckling of angles. If

yielding starts at the ends the bending stiffness of these portions ξL (Fig. 10a) is reduced very drastically (in the ratio $E_{st}/E = 8/300$). Hence after these portions have reached a certain length the column may be considered as being simply supported. Fig. 13 shows that the critical L/r - ratio becomes equal to the one of a simply supported column ($L/r = 94.9$) for $\xi = 0.15$, the corresponding critical strain ε_{cr} being about $4.5 \cdot 10^{-3}$. If the L/r - ratio is smaller yielding may progress further on. Then the elastic middle part of the column may be taken as complete rigid compared to the end portions with a greatly reduced bending stiffness $E_{st}I$. Buckling will occur in a shape as shown in Fig. 10d. The critical slenderness ratio is given by

$$\sigma_{cr} = \sigma_y = \frac{\pi^2 E_{st}}{(\xi L/r)^2} \tag{12}$$

or explicity

$$L/r = \frac{\pi}{\xi}\sqrt{E_{st}/\sigma_y} \tag{13}$$

Curves (d) in Fig. 13 allow to compare the approximation with the "exact" solution (curves (a) and (b)). Accordingly a column with $L/r > 94.9$ will buckle as soon as yielding starts ($\xi = 0$). For values $94.9 \geqslant L/r \geqslant 30.8$ the totally yielded zones extend between $0.15 \leqslant \xi \leqslant 0.50$. The "exact" solution avoids the discontinuity at $L/r = 94.8$. Nevertheless the approximation describes the behavior fairly well especially for values $L/r < 94.9$.

3. Torsional Buckling of Angles in the Plastic Range:

After this short and incomplete study of the behavior of columns loaded into the plastic range the case of torsional buckling of axially compressed angle specimens is taken up. The

previously treated problem indicated the possibility of certain simplifications which will be used in the following to make the present problem mathematically treatable.

A fixed-ended angle with equal legs, as shown in Fig. 15a, has a L/r - ratio < 30 such that Euler-buckling will not occur. If the b/t - ratio of the flanges is large enough, the angle may fail torsionally by rotating around its heel. To analyze this type of failure a flange may be looked upon as a plate (Fig. 15b) fixed at its ends $x = 0$ and $x = L$, simply supported along $y = 0$ (no interaction between the flanges) and free along $y = b$. In the elastic range the critical stress of such a plate is:*

$$\sigma_{cr} = \frac{\pi^2 E}{12(1-\nu^2)} (t/b)^2 \left[4(b/L)^2 + 0.425 \right] \qquad (14)$$

If the dimensions of the flange are such that σ_{cr} would be larger than σ_y (yield stress), yielding will start somewhere in the angle, preferably at the fixed ends. For, due to lateral restraint shear stresses τ_{xy} are present locally at the ends such that their combination with the applied axial stresses σ_x will fulfill the yield condition before σ_x reaches σ_y. Such a behavior was shown by all specimens reported on in the first part of this paper. Yielding reduces the effective modulus of these end zones ξL (Fig. 15b) to the strain hardening modulus E_{st} such that the flange may be considered simply supported along the two edges $x = 0$ and $x = L$. The critical stress of such a plate becomes:**

---

* See reference (8), eq. (10). Proper adjustment for $\nu = 0.3$ has been made.

Note: Due to the fact that shear center and centroid of such a cross-section are not identical torsional buckling may be accompanied by bending about the strong axis such that the resulting critical load will be reduced. However, for short specimens this influence is practically negligible (See reference (4), p. 132-36)

** See reference (7), p. 338, $\nu = 0.30$.

$$\sigma_{cr} = \sigma_y = \frac{\pi^2 E}{12(1-\nu^2)} \cdot (t/b)^2 \left[(b/L)^2 + 0.425 \right] \qquad (15)$$

The only term affected with respect to eq. (14) is the b/L - term in which the 4 dropped out. It should be understood that this equation is approximate. But the previous example of the fixed-ended column shows that it may describe sufficiently the actual behavior.

Assume now the ratios b/t and b/L are such that eq.(15) is still not satisfied, yielding will spread further toward the middle. The middle section, being still elastic, is practically rigid compared to the yielded zones ξL such that only the later will deform if buckling occurs (Fig. 15c).

Following Bleich's semi-rational approach to the problem of plate buckling in the plastic range*, the effective modulus of a completely yielded zone becomes E_{st} in direction of the applied stress (x-direction). In a direction perpendicular to it (y-direction) it remains at its elastic value E. The shearing modulus lays somewhere between its elastic and plastic value; quite arbitrarily it is taken to $\sqrt{\tau}\,G$, where $\tau = E_t/E$ (tangent modulus/modulus of elasticity). Modern theories of Plasticity [2], [3] will challenge such assumptions as arbitrary. Numerous tests were made by many investigators on the stress-strain relations in the region of initial yielding or on continuously strain-hardening materials. Laws derived from such tests can not be applied to a material yielding in very thin layers in which the strains "jump" from their elastic to strain hardening values. Experimental data on material such as A-7 steel are badly needed. For the time being the above made assumptions appear to be as

* See reference [4], p. 307

good as any.

At this place another difficulty may be mentioned. The experimental determination of the strain hardening modulus E_{st} is so much more difficult than the one of the modulus of elasticity E. More precisely, its value may change considerably from one specimen to another. E_{st} is not a material property showing the same consistency as E. For practical purposes it may become necessary to fix a lower limit, as it is done for the yield stress of steel, and work with this value.

Summarizing, the following assumption were introduced:

1. The two end zones ξL are yielded all the way to the strain hardening range (Fig. 15b). The middle zone $L(1-2\xi)$ is still elastic.
2. If buckling takes place only the end zones will deform, the middle zone can be considered to be rigid (Fig. 15c).
3. The yielded zones become anisotropic such that the effective moduli become:

x - direction: E_{st}

y - direction: E

Shearing Modulus: $\sqrt{E_{st}/E}\ G$

Buckling of the yielded parts then occurs for:

$$\sigma_{cr} = \sigma_y = \frac{\pi^2 E_{st}}{12(1-\nu^2)} (t/b)^2 \left[(b/\xi L)^2 + 0.425 \right] \qquad (16)$$

This equation allows the determination of the extension of the yielded zones ξL knowing the yield stress σ_y, the modulus of elasticity E, the strain hardening modulus E_{st} and the b/t - ratio of the plate. The total shortening of the plate and the average strain at which buckling will occur are calculated in exactly the same manner as for the columns treated previously.

Hence eq. (6) still applies for ε_{cr}:

$$\varepsilon_{cr} = (1-2\xi)\,\varepsilon_y + 2\xi\varepsilon_{st} \qquad (6)$$

Fig. 16 and 17 show graphically the results of b/t vs ξ and $\varepsilon_{cr}/\varepsilon_y$ vs b/t. For their derivation the following material properties, corresponding to mean values of the annealed material of the tested angle specimens, were used:

$$\sigma = 34{,}500 \text{ psi}$$

$$E = 30\cdot10^6 \text{ psi}$$

$$E_{st} = 9\cdot10^5 \text{ psi}$$

$$\varepsilon_y = 1.15\cdot10^{-3}$$

$$\varepsilon_{st} = 13\cdot10^{-3}$$

The b/L ratio of all specimens was practically constant (see Table I) such that b/L = 1/5.35 was used for the computations. Incidentally, in Fig. 17 other curves are shown which were computed according to the theories in reference (2), (3), (4). Their derivations will be given afterwards.

The results of the 8 tests are plotted in Fig. 17. It is clearly evident that the magnitude of the critical strain increases rather suddenly around b/t=9. Below b/t=8 the critical strain reaches into the strain-hardening range.

The influence of the $(b/\xi L)$ - term in eq. (16) is rather small. For the limiting case $\xi = 0.5$, i.e. yielding takes place in its full extent over the entire length L, eq. (16) together with the above given values leads to the critical b/t - ratio = 8.04. Neglecting the $(b/\xi L)$ - term reduces it to b/t = 7.81, the difference between these to values being only 3%. It then appears that a freely supported flange with a b/t - ratio $\lesssim$ 7.81 can be strained at least to the strain hardening strain ε_{st} before it buckles. Such a behavior is desired in "Plastic Design" where

the "hinges" must sustain considerable strains to arrive at the assumed equalization of the moments.

4. Comparison with Plastic Buckling Theories:

The 3 types of theories as presented in references (2), (3), (4) make the common assumption that yielding is a "quasi-homogeneous" process. Hence yielding in an axially compressed specimen will start over its entire length, the local strains will grow continuously. This may be the case for certain alloys. On the other hand structural steel of the A-7 type shows a completely different behavior as was pointed out before. Once more the stress-strain curve as shown in Fig. 8 is deceiving and does not apply for local strains.

Stowell's theory (2) applied to a long flange with one unloaded edge simply supported leads to the following buckling condition:

$$\sigma_{cr} = \frac{\pi^2 \eta E}{12(1-\nu^2)} (t/b)^2 \cdot 0.425$$

$$\eta = E_s/E$$

$$E_s = \text{Secant Modulus}$$

For a flange of finite length L the b/L - term enters such that for a plate as shown in Fig. 15b the above condition change to:

$$\sigma_{cr} = \frac{\pi^2 \eta E}{12(1-\nu^2)} (t/b)^2 \left[4(b/L)^2 + 0.425\right]$$

This is an approximation only, as $4(b/L)^2$ should be multiplied by a constant <1. The evaluation of this constant is quite involved and is omitted here as the influence of this term is very small. The above equation leads to b/t - values slightly above the "exact" solution. Dividing both sides by E_s gives

$$\varepsilon_{cr} = \frac{\sigma_{cr}}{E_s} = \frac{\pi^2}{12(1-\nu^2)} (t/b)^2 \left[4(b/L)^2 + 0.425\right] \qquad (17)$$

In Fig. 17 $\varepsilon_{cr}/\varepsilon_y$ as function of b/t is shown.

An analysis along the line of the Handelman-Prager theory (2) shows that for the problem at hand the shearing modulus would keep its elastic value after yielding has been reached such that*

$$\sigma_{cr} = \sigma_y = \frac{\pi^2 E}{12(1-\nu^2)} (t/b)^2 \cdot 0.460 \qquad (18)$$

Furthermore a discontinuity at yielding occurs (their D_{11}^{-1} jumps from 1 to 0.238 influencing the b/L - term). Substituting the numerical values on p. 18 results in

$$b/t = 19$$

Formulated in words, the theory gives the following results: Right below σ_y = 34,500 psi the critical b/t = 21, at yielding b/t = 19 and for b/t < 19 the plate will carry the strain into the strain-hardening range (see Fig. 17).

Bleich (4) gives the following equation for the present problem:

$$\sigma_{cr} = \frac{\pi^2 \sqrt{\tau}\, E}{12(1-\nu^2)} (t/b)^2 \left[4(b/L)^2 + 0.425 \right] \qquad (19)$$

After yielding occurred the tangent modulus E_t is zero such that eq. (19) does not lend itself to a solution. As in the case of columns (eq. (1)) a solution becomes formally possible if the strain reaches the strain-hardening range ε_{st} and E_t becomes equal to the strain hardening modulus E_{st}.

An inspection of Fig. 17, showing the test results and the predictions of the different theories, permits the following conclusions:

1. The theory presented by Handelman-Prager does not describe the problem at hand. The reason may well be that their stress-strain laws in the presented form cannot be

---

* Eq. (18) is derived from Eq. (151) of reference (3)

applied to structural steel under uni-axial compression.

2. Bleich's equation gives solutions only up to $E_t = 0$, i.e. up to the yield level. Its direct application to the case $E_t = E_{st}$ is arbitrary. For no explanation is given in which manner the strain can reach the strain hardening zone.

3. Qualitatively, Stowell's theory does not follow the manner in which yielding of the tested specimens occurred. Whereas it presupposes yielding to take place more or less uniformly all along the length of the specimen, it actually was concentrated toward the ends and started to spread from there. Quantitatively, it seems to give too conservative results in the range near the strain hardening zone. This zone is important in specifying such b/t - ratios of flanges that no local buckling will occur if they are strained far into the plastic range. This is exactly the ultimate aim of the present investigation.

4. The theory advanced in this paper tries to take into account the discontinuity in the yielding process. It illustrates the manner in which a specimen with a sufficiently small b/t - ratio ($b/t < 8$) may overcome the yield level such that Bleich's formula (equation (19)) becomes again applicable. The test results are too few to make any final conclusions.

Much remains to be done to arrive at a rational buckling theory which is applicable to plates of mild steel in the plastic range. Especially experimental values on the effective moduli in direction of the applied stress, perpendicular to it and in shear are necessary. Due consideration must be given to the fact that yielding occurs discontinuously and non-homogeneously.

ACKNOWLEDGEMENTS

This work has been carried out at Fritz Engineering Laboratory as a partial study of the project "Welded Continuous Frames and Their Components", sponsored by the Welding Research Council and the Department of the Navy, with funds provided by the American Institute of Steel Construction, the American Iron and Steel Institute, the Office of Naval Research, the Bureau of Ships and the Bureau of Yards and Docks. The project is under the direction of Dr. L. S. Beedle.

The authors wish to express their appreciation to Mr. A. T. Gozum for his cooperative help in testing the specimens, working up the experimental data and preparing the drawings of the present report.

List of References

(1) Yang, C. H., Beedle, L. S. "Inelastic Local Buckling of WF Sections" Progress Report Q, Fritz Lab., Lehigh University, May 1, 1952

(2) Stowell, E. Z. "A Unified Theory of Plastic Buckling of Columns and Plates", NACA, Report No. 898, 1948

(3) Handelman, G. H., Prager, W. "Plastic Buckling of Rectangular Plates Under Edge Thrusts", NACA, T.N. 1530, August 1948

(4) Bleich, F. "Buckling Strength of Metal Structures" McGraw-Hill, New York, 1952

(5) Nadai, A. "Theory of Flow and Fracture of Solids" McGraw-Hill, New York, 1950

(6) Haaijer, G. "Compression Tests on Short Steel Columns of Rectangular Cross-Section", Progress Report S, Fritz Lab., Lehigh University, June 1953

(7) Timoshenko, S. "Theory of Elastic Stability", McGraw-Hill, New York, 1936

(8) Hill, H. N. "Chart for Critical Compressive Stress of Flat Rectangular Plates", NACA, T. N. 773, August 1940

TABLE I

DIMENSIONS OF SPECIMENS

Specimen	Material	Length L (in.)	Width b (in.)	Thickness, t (in.)	b/t	L/b	Area (in2)
A-21	Annealed	25.0	4.87	0.383	12.70	5.14	3.78
A-22	Annealed	25.0	4.79	0.381	12.60	5.21	3.70
A-31	Annealed	17.9	3.27	0.370	8.85	5.48	2.48
A-32	Annealed	17.9	3.28	0.374	8.79	5.46	2.51
A-41	Annealed	12.5	2.31	0.377	6.13	5.41	1.80
A-42	Annealed	12.5	2.34	0.371	6.36	5.35	1.81
A-33	As-Delivered	17.5	3.30	0.378	8.73	5.30	2.55
A-51	As-Delivered	21.2	4.07	0.380	10.70	5.21	3.15

Table II

Buckling Stress σ_{cr} and Buckling Strain ϵ_{cr} Specimens

Specimen	Material	b/t	Yield Stress σ_y (ksi)	Buckling Detected by									Maximum Load		Type of Failure
				"Buckling Detector"			SR-4 Strain Gages			Rotation Measurement					
				$\epsilon_{cr} \cdot 10^3$	$\epsilon_{max} \cdot 10^3$	σ_{cr} (ksi)	$\epsilon_{cr} \cdot 10^3$	$\epsilon_{max} \cdot 10^3$	σ_{cr} (ksi)	$\epsilon_{cr} \cdot 10^3$	$\epsilon_{max} \cdot 10^3$	σ_{cr}	$\epsilon \cdot 10^3$	σ_{max} (ksi)	
A-21	Annealed	12.70	33.1	2.8*	12.1 +	32.2	3.3	14.3 +	31.8		n.m.		1.2	33.1	Torsional
A-22	Annealed	12.60	32.3	3.0	12.3 +	32.5	2.8	12.3 +	31.5	2.6*	12.3 +	32.8	1.31	33.1	Torsional
A-31	Annealed	8.85	34.9	16.5	out	36.0	All gages out before Strain Deviation			12.5*	n.m.	34.4	18.4	36.5	Torsional
A-32	Annealed	8.78	34.6	15.7	out	35.3				12.8*	15.3	34.6	17.5	35.6	Torsional
A-41	Annealed	6.13	35.3	No Indication			No Strain Deviation			No Rotation n.r.			43.9	42.8	Column Buckling
A-42	Annealed	6.26	34.1										32.8	43.6	Column Buckling
A-33	As Delivered	8.73	41.3	n.m.			13.2	n.m.	45.5	14.7*	n.m.	46.2	16.7	48.4	Torsional with bending about Weak Axis
A-51	As Delivered	10.70	41.0	n.m.			7.6	n.m.	44.5	2.8*	4.1	47.0	7.0	41.6	Torsional

* – Plotted in Fig. 4 Indicating Torsional Buckling

\+ – Irregular

n.m. – Not measured

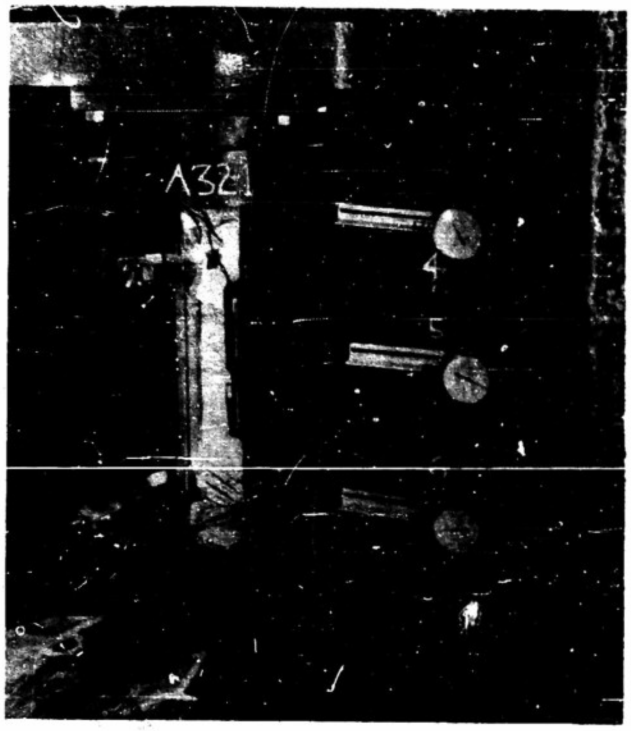

$\varepsilon = 2.94 \times 10^{-3}$

$\sigma = 34.6$ ksi

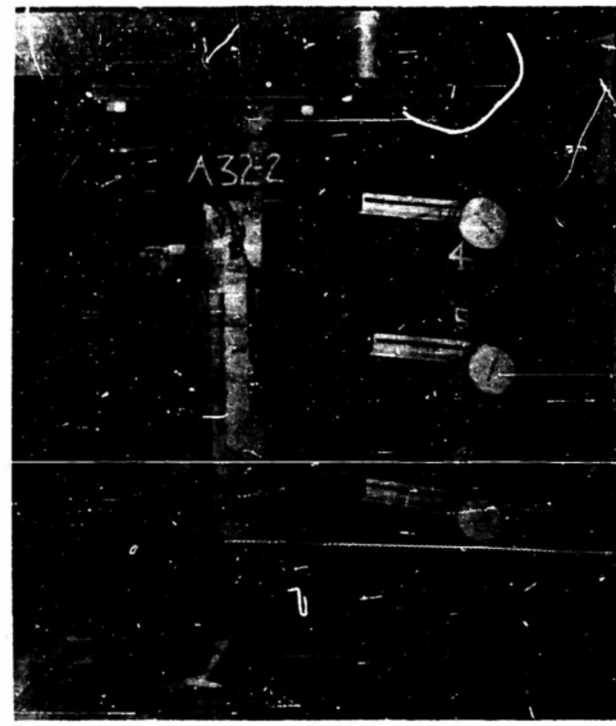

$\varepsilon = 6.15 \times 10^{-3}$

$\sigma = 34.6$ ksi

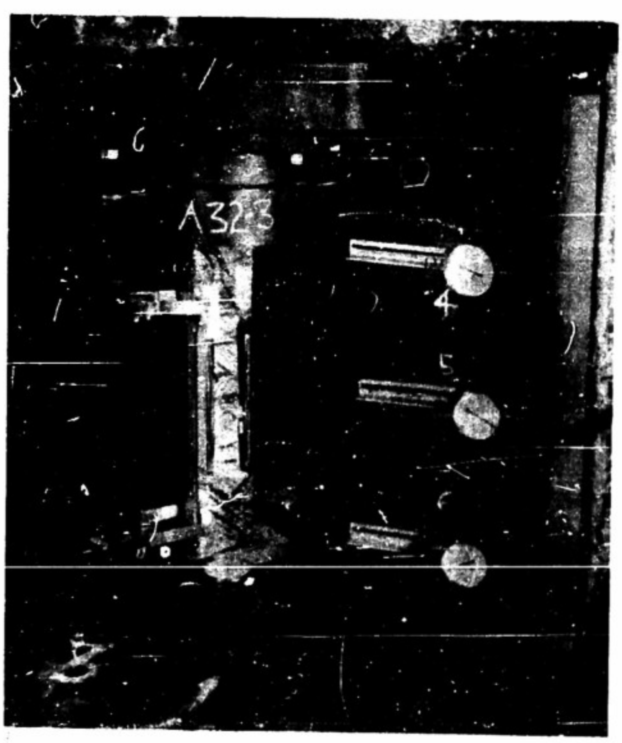

$\varepsilon = 12.82 \times 10^{-3}$

$\sigma = 34.70$ ksi

$\varepsilon = 25.53 \times 10^{-3}$

$\sigma = 30.80$ ksi

Fig. 1 TEST OF SPECIMEN A-32

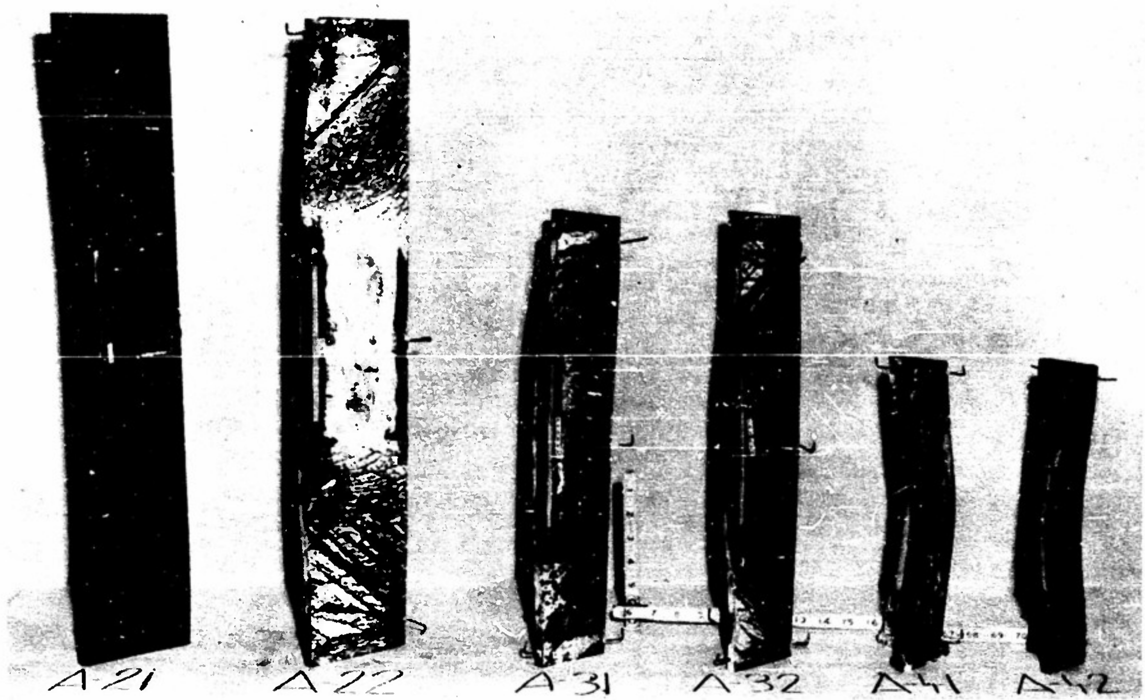

Fig. 2a - Annealed Specimens after Testing
Showing Deformation of the Heel

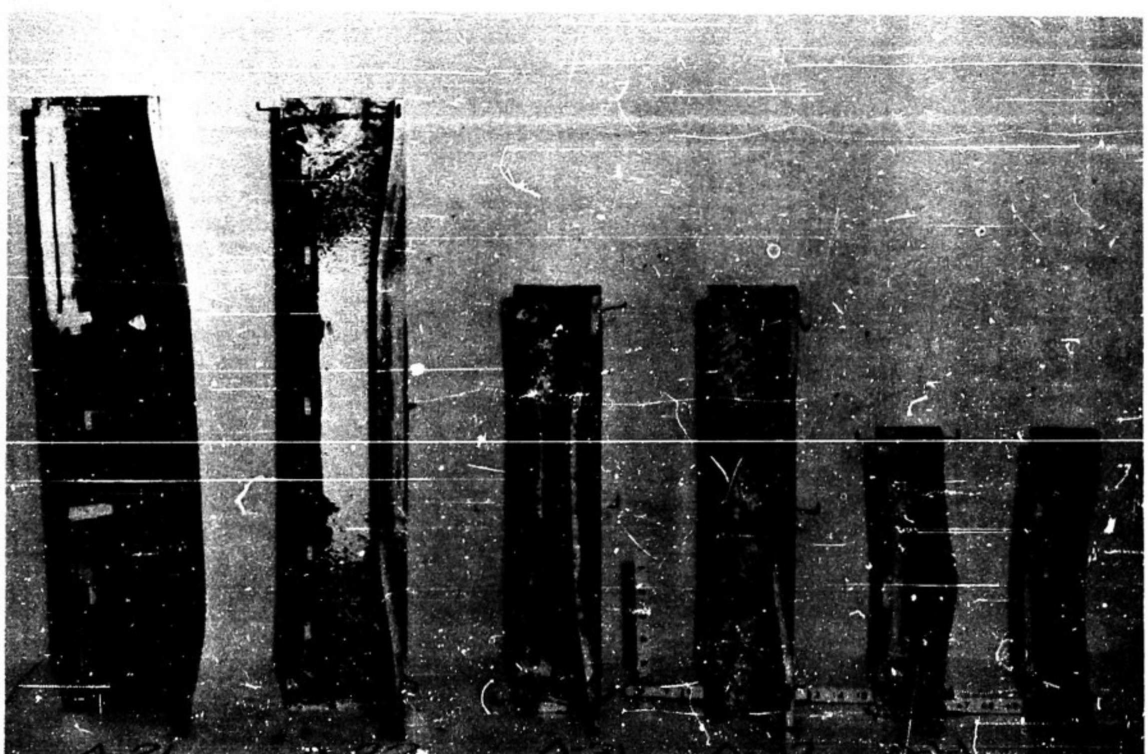

Fig. 2b - Annealed Specimens after Testing
Showing Buckled Flanges

205 E-3

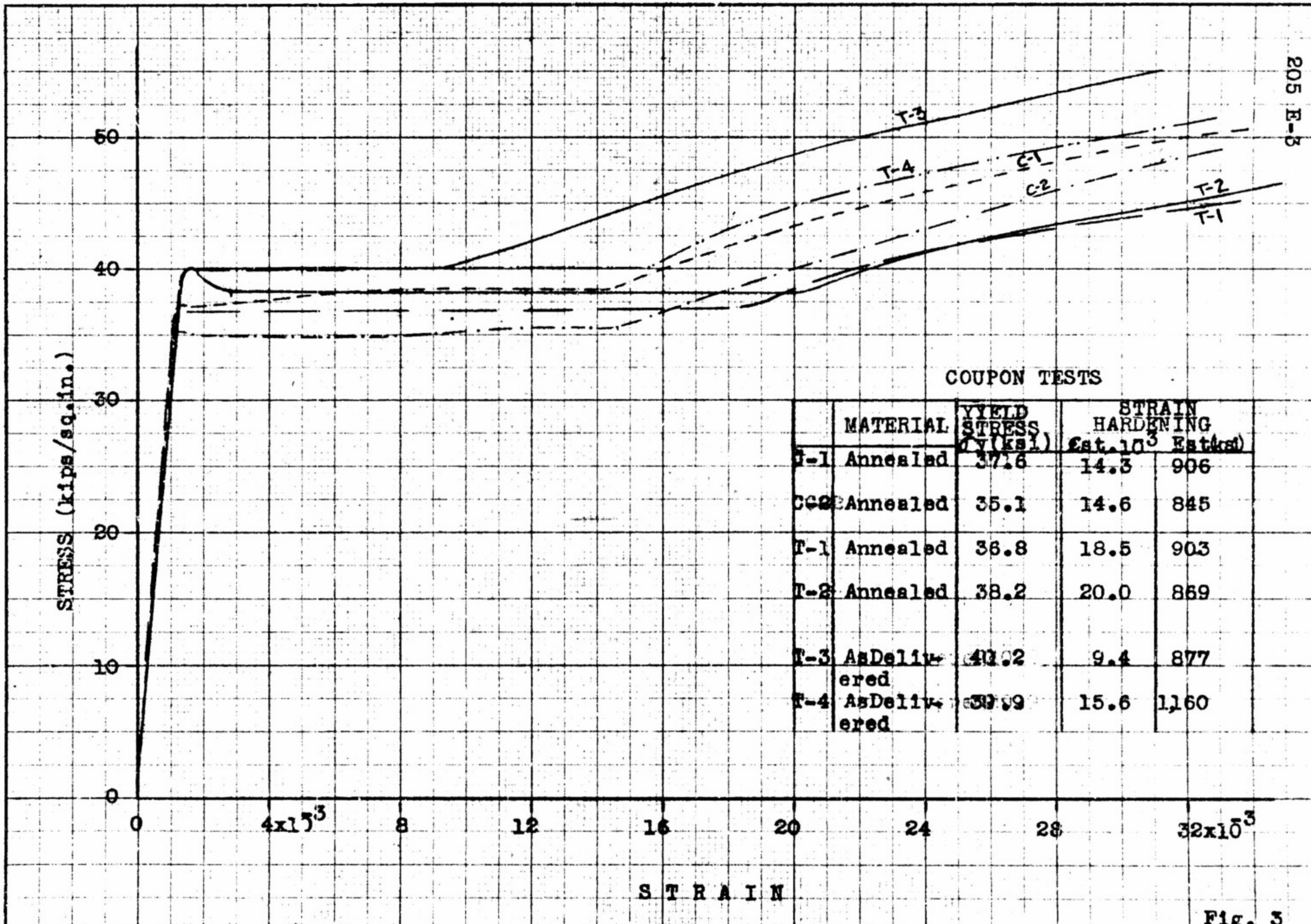

COUPON TESTS

	MATERIAL	YIELD STRESS σ_y (ksi)	STRAIN HARDENING $\epsilon_{st} \cdot 10^3$	E_{st} (ksi)
C-1	Annealed	37.6	14.3	906
C-2	Annealed	35.1	14.6	845
T-1	Annealed	36.8	18.5	903
T-2	Annealed	38.2	20.0	869
T-3	As Delivered	40.2	9.4	877
T-4	As Delivered	39.9	15.6	1,160

Fig. 3

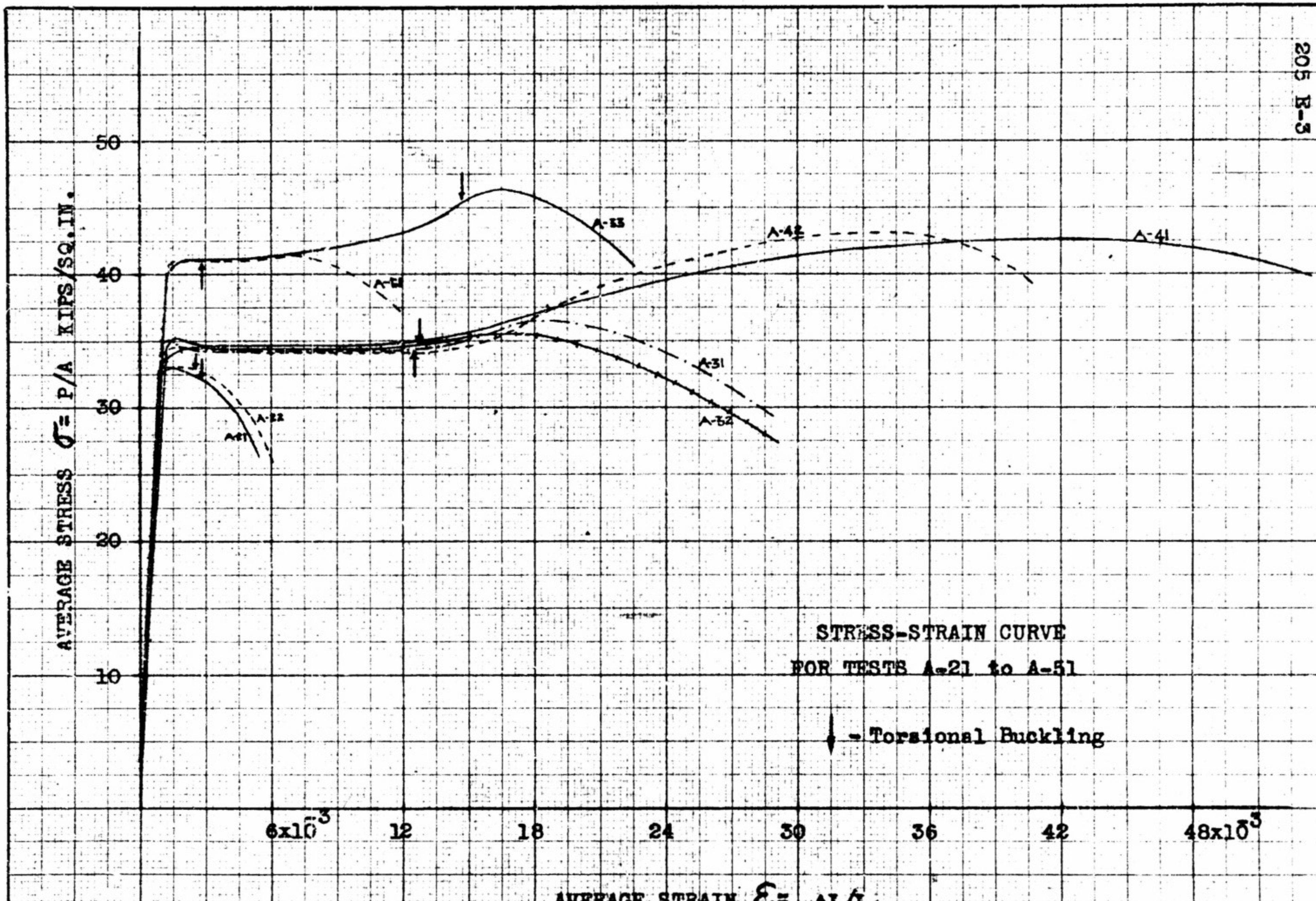
205 E-3
50
40
30
20
10
6x10^{-3}
12
18
24
30
36
42
48x10^{-3}
AVERAGE STRESS σ = P/A KIPS/SQ.IN.
AVERAGE STRAIN ε = ΔL/L
A-33
A-42
A-41
A-31
A-32
A-22
A-21
STRESS-STRAIN CURVE
FOR TESTS A-21 to A-51
- Torsional Buckling

Fig. 4

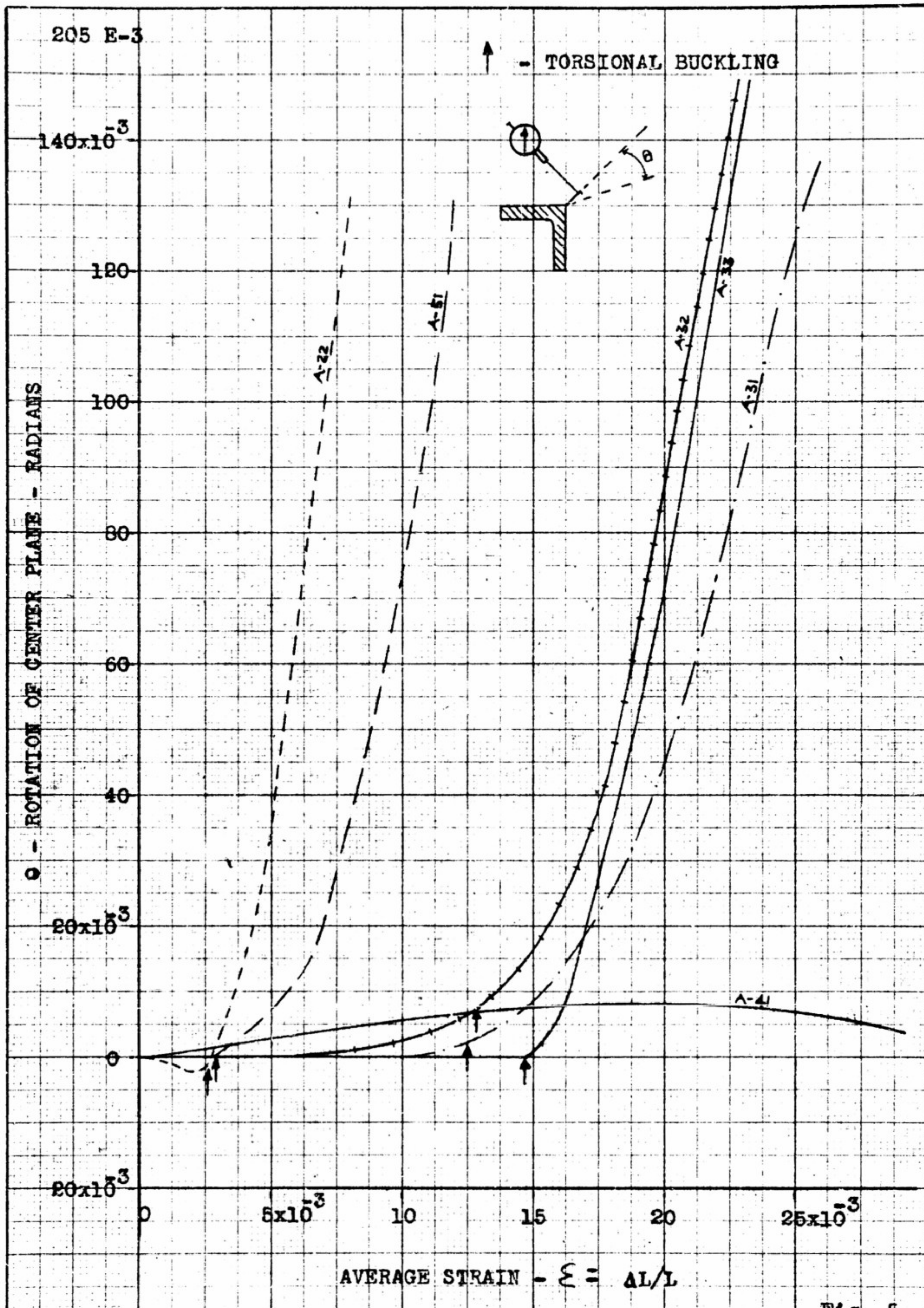
205 E-3
↑ - TORSIONAL BUCKLING
θ
140x10^-3
120
100
80
60
40
20x10^-3
0
20x10^-3
θ - ROTATION OF CENTER PLANE - RADIANS
A-22
A-51
A-32
A-33
A-31
A-41
0
5x10^-3
10
15
20
25x10^-3
AVERAGE STRAIN - ε = ΔL/L
Fig. 5

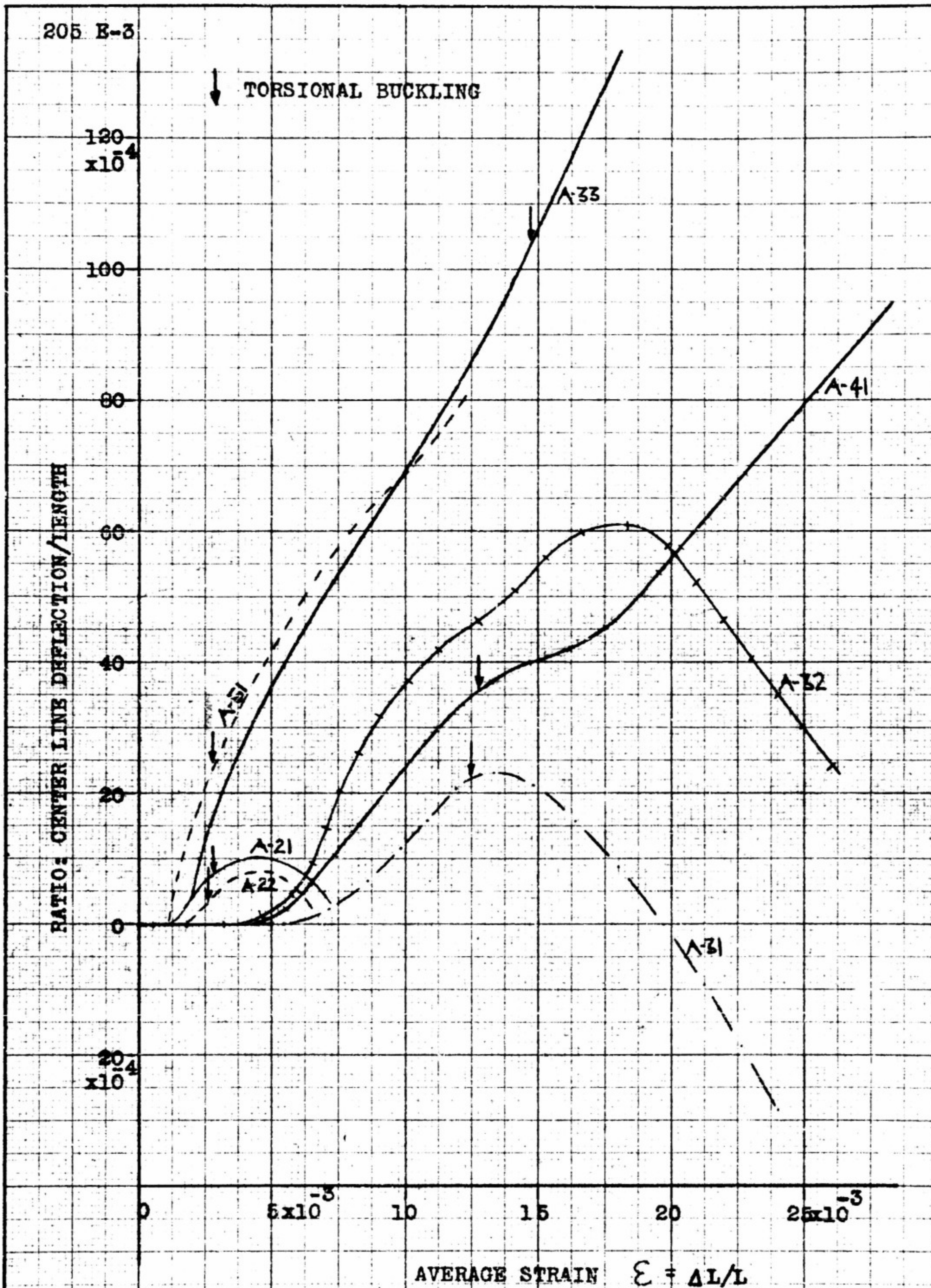
205 E-3
TORSIONAL BUCKLING
120 x10^-4
100
80
60
40
20
0
20 x10^-4
RATIO: CENTER LINE DEFLECTION/LENGTH
A-33
A-41
A-32
A-31
A-21
A-22
0
5x10^-3
10
15
20
25x10^-3
AVERAGE STRAIN ε = ΔL/L

Fig. 6

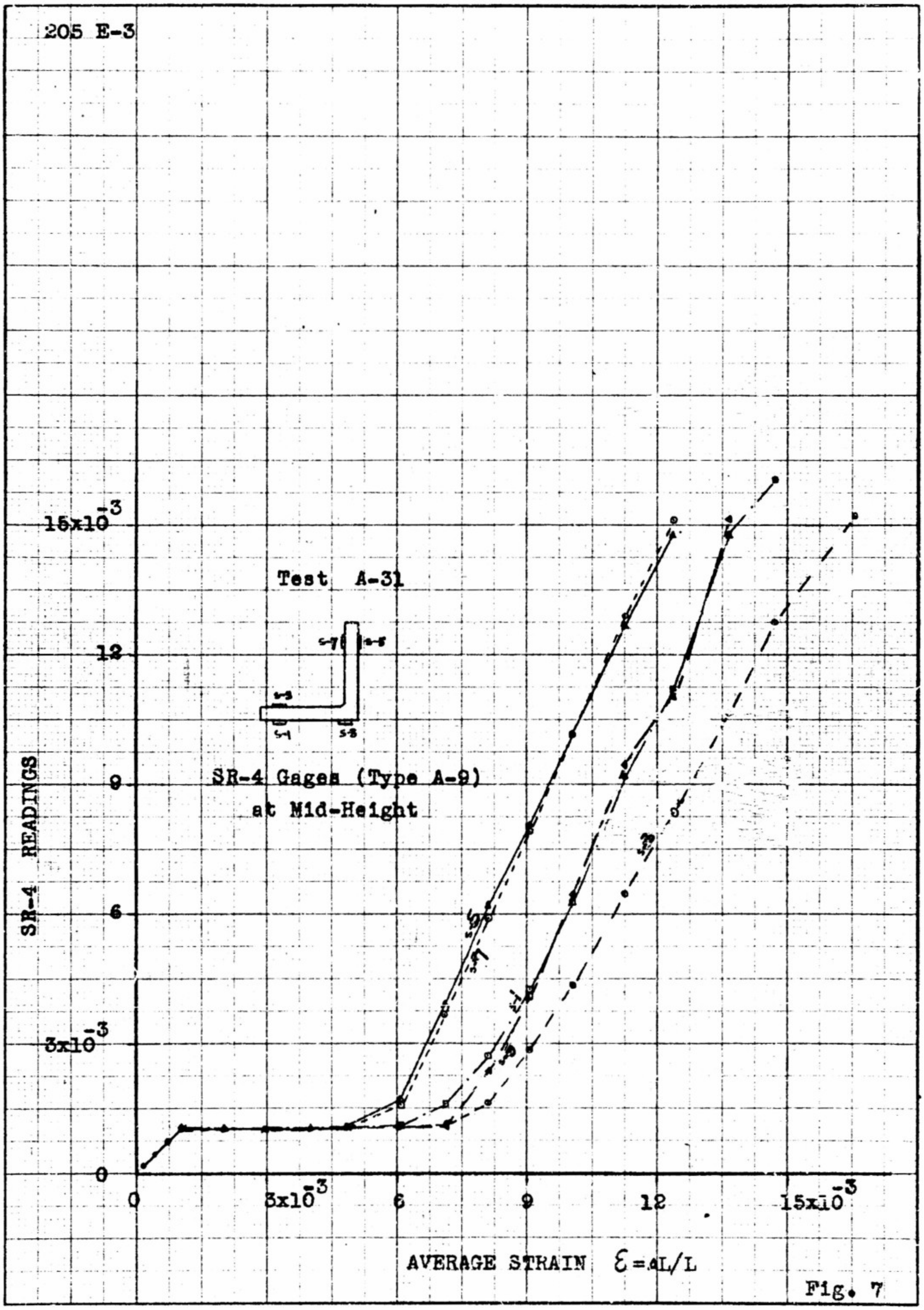

205 E-3
Test A-31
SR-4 Gages (Type A-9)
at Mid-Height
SR-4 READINGS
15x10^-3
12
9
6
3x10^-3
0
0
3x10^-3
6
9
12
15x10^-3
AVERAGE STRAIN ε = ΔL/L

Fig. 7

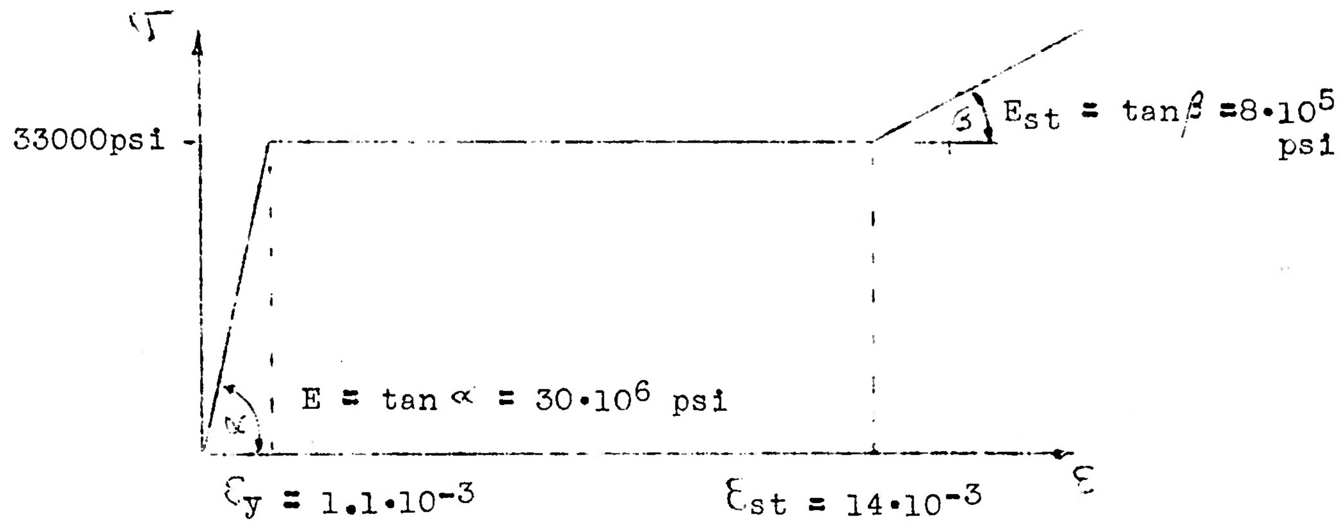

Fig. 8

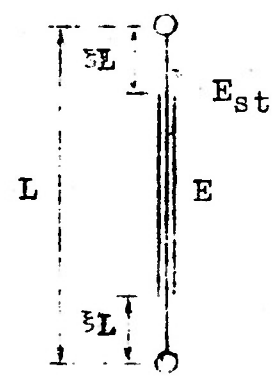

Fig. 9a

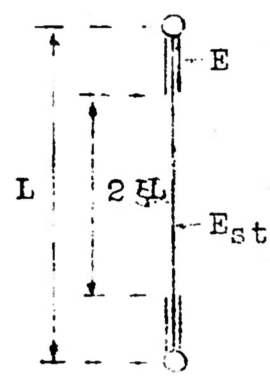

Fig. 9b

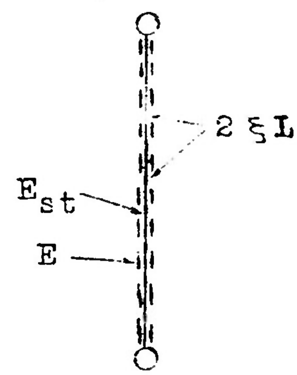

Fig. 9c

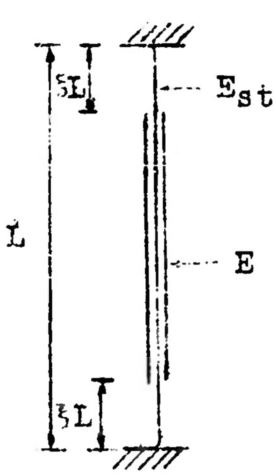

Fig. 10a

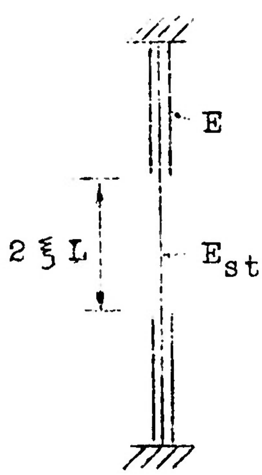

Fig. 10b

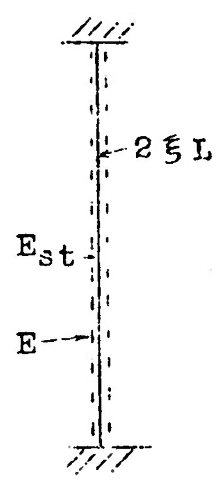

Fig. 10c

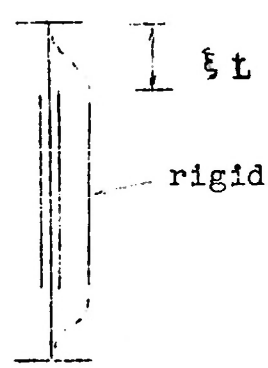

Fig. 10d

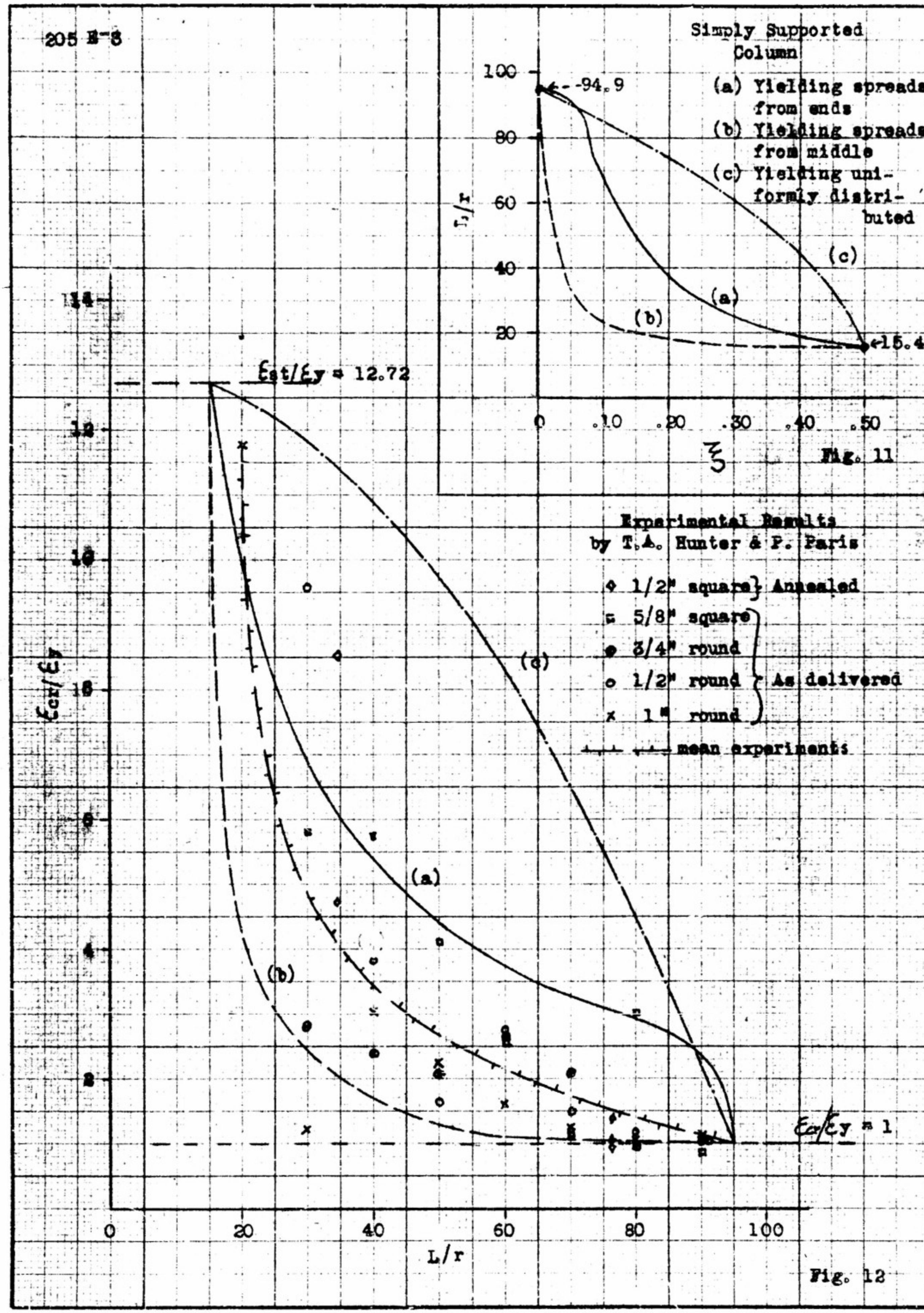

Simply Supported Column
(a) Yielding spreads from ends
(b) Yielding spreads from middle
(c) Yielding uniformly distributed
-94.9
15.4
L₁/r
ξ
Fig. 11
Est/Ey = 12.72
Ecr/Ey
Ecr/Ey = 1
(a)
(b)
(c)
Experimental Results by T. A. Hunter & P. Paris
1/2" square } Annealed
5/8" square
3/4" round
1/2" round } As delivered
1" round
mean experiments
L/r

Fig. 12

205 E-3

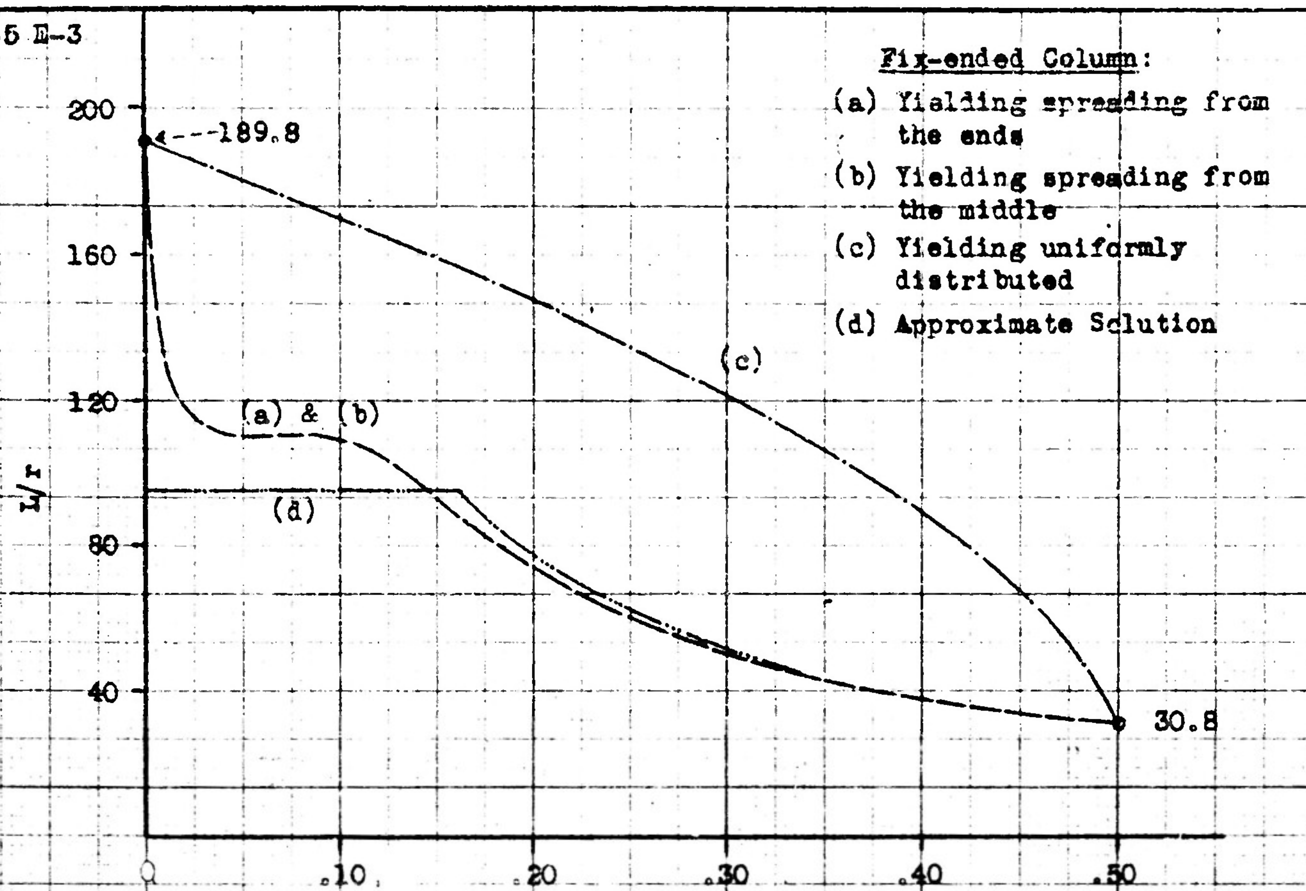

Fig. 13

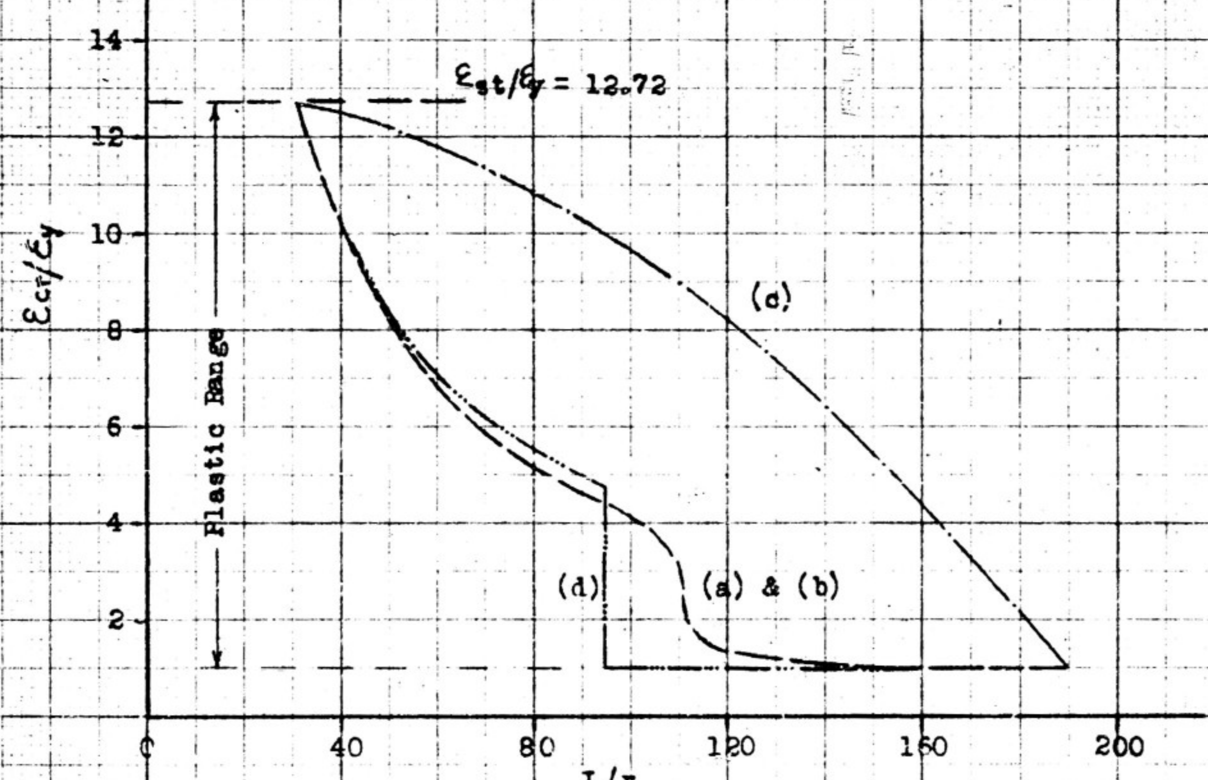

Fig. 14

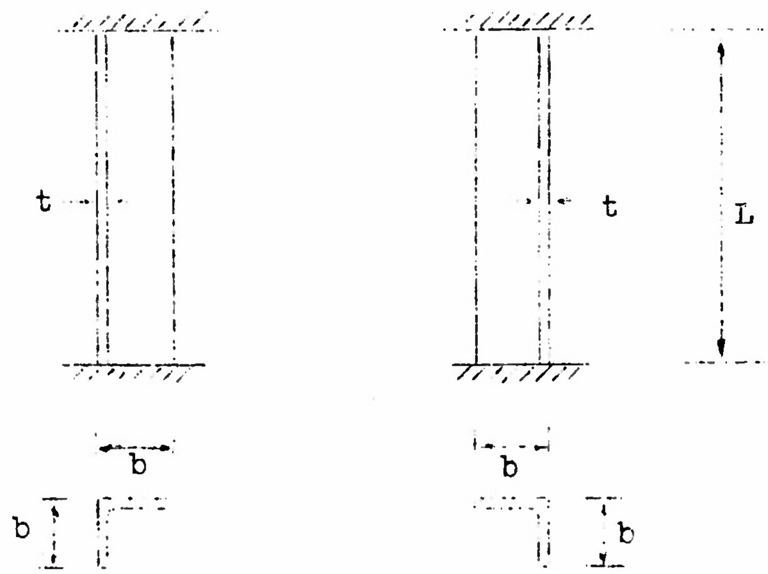

Fig. 15a

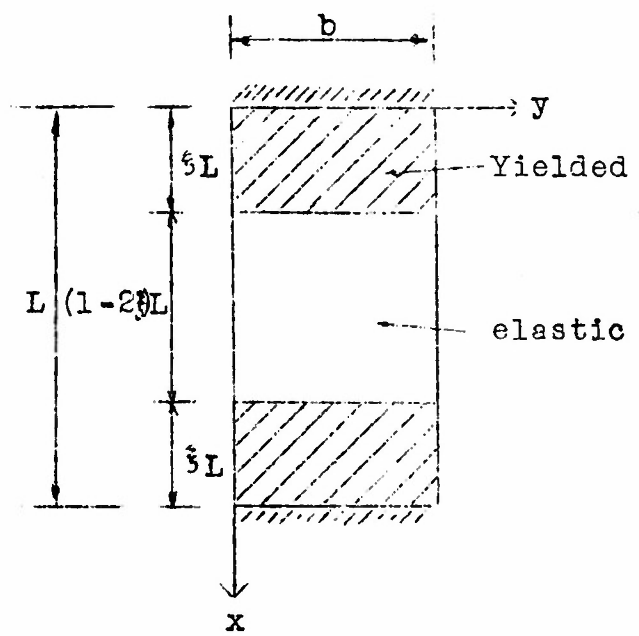

Fig. 15b

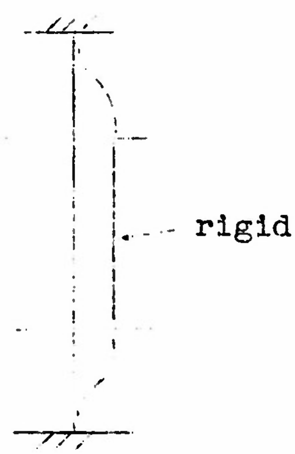

Fig. 15c

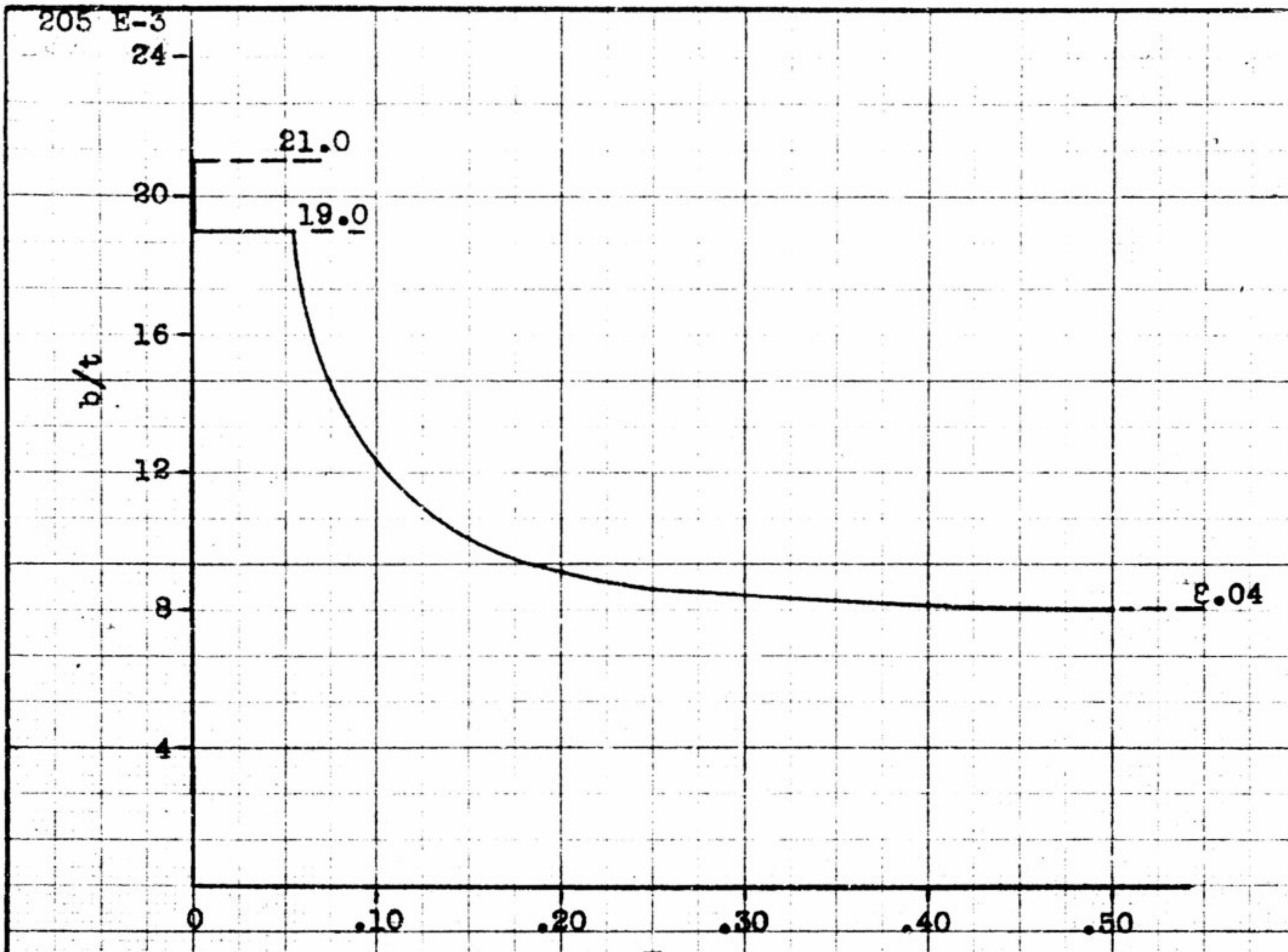
205 E-3
24
21.0
20
19.0
16
b/t
12
8
8.04
4
0
.10
.20
.30
.40
.50
ξ

Fig. 16

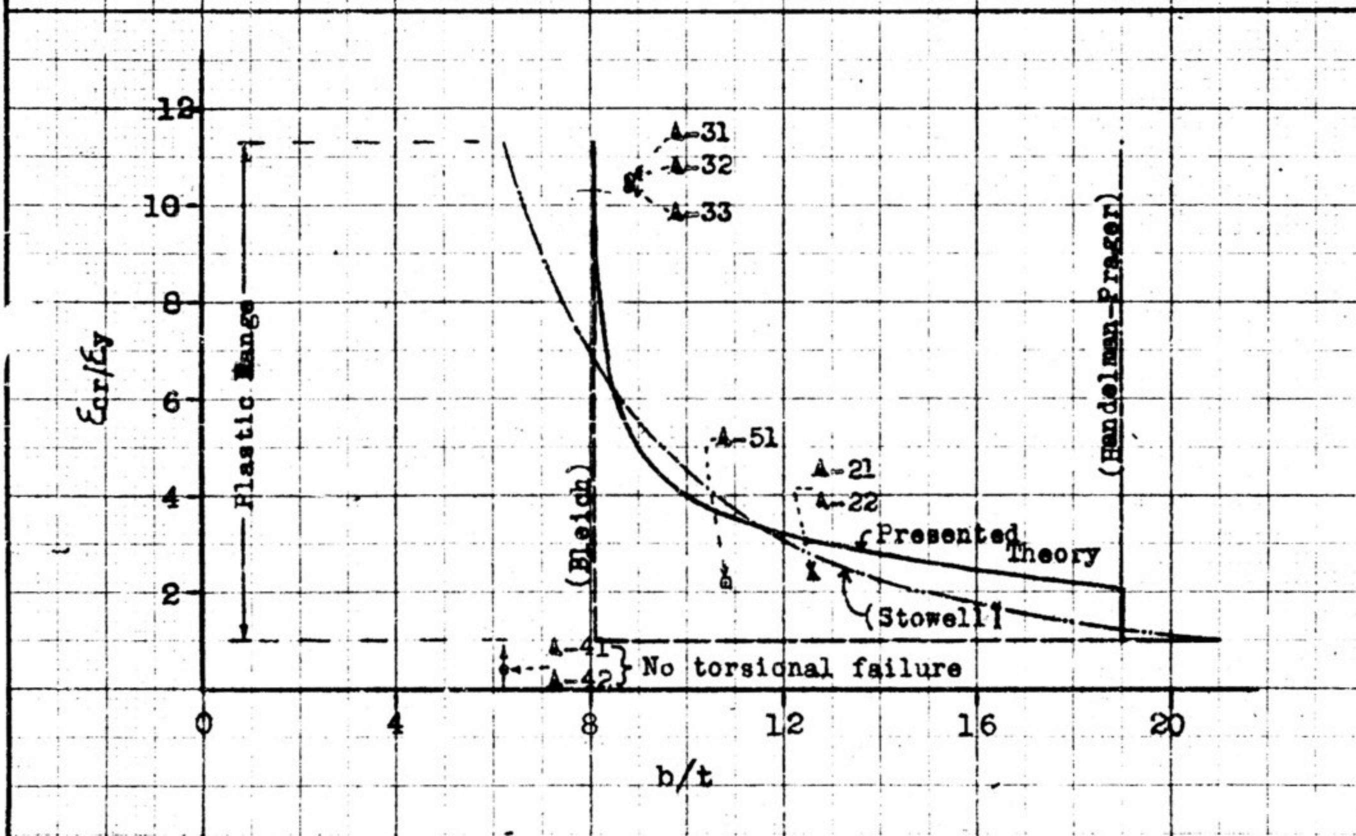
12
10
8
6
4
2
$\mathcal{E}_{cr}/\mathcal{E}_y$
Plastic Range
A-31
A-32
A-33
A-51
A-21
A-22
(Bleich)
Presented Theory
(Stowell)
(Handelman-Prager)
A-41
A-42
No torsional failure
0
4
8
12
16
20
b/t

Fig. 17